COMMUNICATION

Photo-tuning of highly selective wetting in inverse opals†

Thomas A. Singleton,[a] Ian B. Burgess,*[b] Bryan A. Nerger,[bc] Alexis Goulet-Hanssens,[a] Natalie Koay,[b] Christopher J. Barrett[a] and Joanna Aizenberg[bd]

Crack-free inverse opals exhibit a sharply defined threshold wettability for infiltration that has enabled their use as colourimetric indicators for liquid identification. Here we demonstrate direct and continuous photo-tuning of this wetting threshold in inverse opals whose surfaces are functionalized with a polymer doped with azobenzene chromophores.

Introduction

Adaptive materials, those whose microscopic or macroscopic properties can adapt to environmental stimuli, are integral components of many classes of emerging technologies, including sensors and indicators,[1,2] drug-delivery systems,[3] submillimetre-scale motors,[4] self-healing materials,[5] building materials,[6] and clothing[7] that adjust their characteristics to ambient conditions (*e.g.* weather). Materials with stimuli-responsive surface energy and/or fluidic properties have potential for widespread use in micro- and nano-scale devices.[8,9] At these scales, well below the capillary length of most liquids, surface forces are large compared to many other interactions (*e.g.* gravity) and surface effects contribute centrally to device performance.[10] Therefore, the ability to dynamically control surface interactions is integral to many micro- and nano-scale device functions in settings ranging from microfluidics to microscale robots and motors.[11,12] Driven by this motivation, numerous classes of materials have been developed whose surface energy is responsive to a variety of different physical and chemical stimuli.[11]

Using light as a stimulus is particularly useful in a number of settings. For devices that interface with biological materials, light places fewer limitations on the target system compared to most other chemical and physical stimuli (*e.g.* pH, electric fields) because it is minimally invasive and universally abundant.[13] The abundance of light is also advantageous for other applications such as microscale locomotion.[14] Numerous materials are currently known to exhibit photo-induced changes in surface energy, including titania[11] and surfaces coated with a variety of photo-active organic molecules or polymers, such as those belonging to the azobenzene[15–17] or spiropyran[18] families. While there has been tremendous progress in the development of photo-responsive surfaces, device architectures that effectively translate photo-induced changes in surface energy into macroscopic, visible functions are less developed. A significant challenge faced in this aspect of design is that photo-induced changes in surface energy are generally small, with intrinsic contact angles for water typically changing by less than $30°$.[17,19] Application of these materials can be greatly expanded by identifying architectures whereby significant changes in function result from very small changes in surface energy.

Crack-free inverse-opal films (IOFs)[20] have recently emerged as an example of such an architecture, where fluid infiltration is remarkably sensitive to surface energy.[21–23] Owing to the highly symmetric pore structure, the transition from complete non-wetting to complete wetting occurs over a decrease in intrinsic contact angle of only $\sim 3°$.[23] Infiltration of the pores is also associated with a dramatic change in the films' colour, due to refractive index matching between the liquid and the silica IOF matrix. This highly selective wetting, coupled with macroscopic colour changes, has been previously exploited for the production of colourimetric indicators for liquids.[22,23] In this paper, we develop photo-responsive IOFs, in which large visible changes in wetting behaviour and colour are triggered by small, optically induced changes in their surface energy. By functionalizing the air–solid interface with a co-polymer of a hydrophilic electrolyte monomer (acrylic acid) and a hydrophobic chromophore (Disperse Red 1 acrylate), we created IOFs whose wetting

[a] Department of Chemistry, McGill University, Montreal, Quebec, H3A 0B8, Canada

[b] Wyss Institute for Biologically Inspired Engineering, Harvard University, Cambridge, MA 02138, USA. E-mail: ibburges@fas.harvard.edu

[c] University of Waterloo, Waterloo, Ontario, N2L 3G1, Canada

[d] School of Engineering and Applied Sciences and Department of Chemistry and Chemical Biology, Harvard University, Cambridge, MA 02138, USA

threshold could be continuously tuned *via* ultraviolet (UV) or visible light exposure, all while maintaining a high wetting selectivity comparable with literature.[23] Photodegradation of the azobenzene chromophores was responsible for the observed irreversible wetting changes. Thus, these films are capable of sensitively and indelibly recording light exposure history, which can be read out directly through the films' colour upon immersion in simple liquids.

Results and discussion

The pore surfaces of IOFs were functionalized with photoactive surface groups using a layer-by-layer polyelectrolyte deposition.[24] IOFs were first functionalized with (3-aminopropyl)trimethoxy-silane to give them a positive charge in aqueous media. We then deposited a layer of the negatively charged photoactive poly-electrolyte, poly(Disperse Red 1 acrylate-*co*-acrylic acid) (p(DR1A-*co*-AA); 20 mol% Disperse Red 1 acrylate, shown in Fig. 1A:
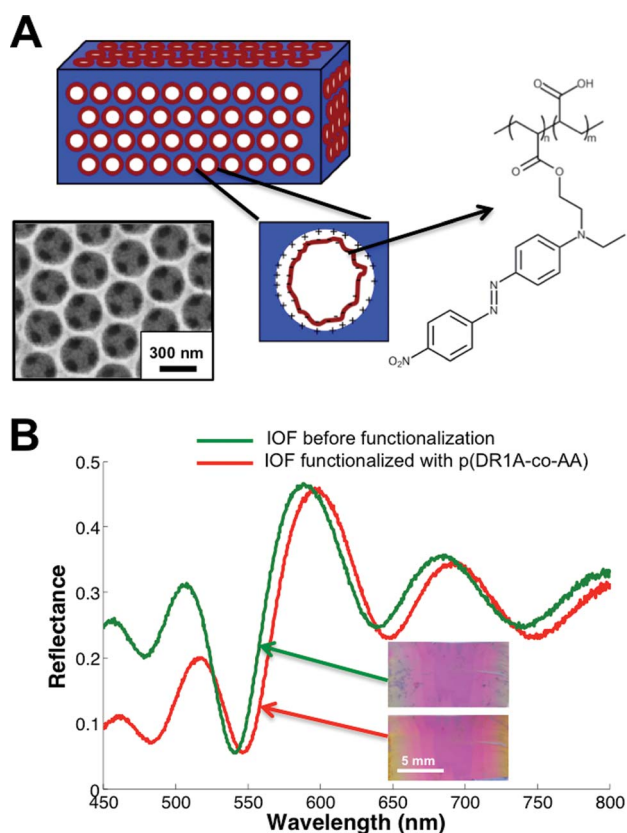

Fig. 1 (A) Schematic depicting the surface functionalization for the inverse-opal film (IOF) pores (scanning electron micrograph of the pore structure is shown at the bottom). The pores were first functionalized with (3-aminopropyl)trimethoxysilane (APTMS) to give them a positive charge in aqueous environments. A layer of the negatively charged polyelectrolyte poly(Disperse Red 1 acrylate-*co*-acrylic acid) was then adsorbed to the pore surfaces. (B) Normal-incidence reflectance spectra for an IOF region with a thickness of 9 close-packed layers before (green) and after (red) functionalization with p(DR1A-*co*-AA), showing suppression of the reflectance by the chromophore in the blue-green region. The inset shows the visual appearance of these films with and without the p(DR1A-*co*-AA) surface coating.

synthesis described in ref. 25). The functionalized IOF displays an enhanced red colour due to light absorption by the chromophore in the blue-green region of the visible spectrum (Fig. 1B). The functionalization preserved the highly selective wetting threshold, characteristic of our IOFs. When immersed in mixtures of water and ethanol with increasing ethanol concentration, IOFs functionalized with p(DR1A-*co*-AA) transitioned from non-wetting to wetting behaviour across a concentration change as small as 2.5% (v/v), as shown in the left column of Fig. 2A (before light exposure). Some variability in the location of this threshold was observed from one sample to the next, with the onset of wetting occurring between 10% and 20% ethanol (by vol), likely owing to small batch-to-batch variations in the pore geometry[23] and the degree of polyelectrolyte coverage.

IOFs functionalized with p(DR1A-*co*-AA) displayed increased hydrophilicity after exposure to UV light (Dymax® Bluewave 200, 280–450 nm). As shown in Fig. 2A, the wetting threshold tuned continuously toward lower ethanol concentrations with increasing UV exposure, while the selectivity of wetting was preserved. Changes in wetting behaviour also occurred uniformly across the exposed regions. After sufficient exposure, all samples underwent wetting by water (see Fig. 2A, far right column). We characterized the magnitude of the photo-induced changes in surface energy by recording the contact angles
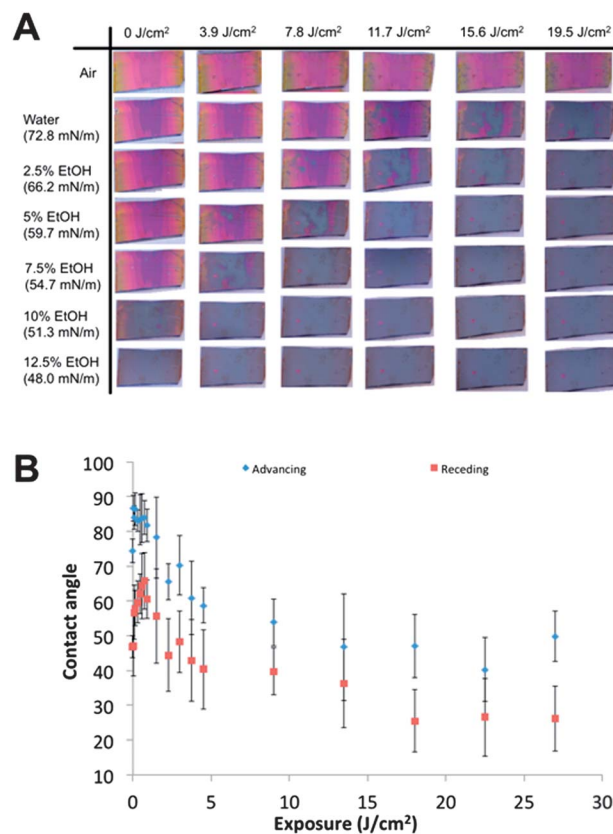

Fig. 2 (A) Wetting response of a p(DR1A-*co*-AA)-functionalized IOF as a function of UV light exposure. For each liquid, surface tensions from ref. 26 are indicated. (B) Advancing and receding contact angles (°) of p(DR1A-*co*-AA)-functionalized flat glass slides as a function of UV exposure.

displayed by water on flat glass slides that were functionalized and exposed to UV in the same manner as p(DR1A-*co*-AA)-functionalized IOFs. Fig. 2B shows the evolution of the advancing and receding contact angles as a function of the UV exposure dose. Advancing contact angles decreased steadily with exposure before stabilizing at ∼20 J cm^{-2}, exhibiting a total decrease of 28 ± 10°. As also noted in previous studies of wetting in IOFs,[21–23] their highly re-entrant geometry causes the onset of imbibition in these structures to occur at intrinsic contact angles well below 90°. It is also worth noting that p(DR1A-*co*-AA)-functionalized surfaces displayed considerable contact angle hysteresis (20–30°) at all doses.

In contrast to other reports of photo-induced changes in surface energy of azobenzene-containing materials, changes to the wetting behavior of these IOFs were irreversible. We found that the changes in IOF wetting behaviour correlated with photobleaching (photodegradation) of the DR1A chromophore, rather than the reversible *cis–trans* isomerization or chromophore alignment effects previously reported.[27] Fig. 3A shows a p(DR1A-*co*-AA)-functionalized IOF in air (top) and submerged in water (bottom) after a large UV exposure dose (>100 J cm^{-2}) was applied to the left portion of the film, qualitatively illustrating the correlation between photobleaching and wetting. The region where water infiltration is occurring (marked by disappearance of colour in the lower image) matches the region where photobleaching has occurred (marked by the change in colour).

Although the exact mechanism of degradation is poorly understood, it likely involves the scission of the N≡N bond, destroying the conjugated electronic structure of the molecule and the strong colouration.[27–29] The correlation between colour changes and changes in wetting behaviour are quantified in Fig. 3B and C for a fixed location in the top left-hand corner of the sample shown in Fig. 2A (IOF thickness of 9 close-packed layers). Fig. 3B shows the evolution of the normal-incidence reflection spectrum in air as a function of UV exposure dose and Fig. 3C shows the spectrum of the same region when the film is submerged in water. Before exposure, reflection is suppressed in the blue-green region by the chromophore absorption (see Fig. 1B). This suppression is most evident for the reflection maximum near 510 nm (to the left of the main reflection peak), whose peak height is reduced to 60% of its original value after functionalization (Fig. 1B). The recovery of this peak with UV exposure can be used as a measure of the degree of photobleaching. Comparing the range of exposure over which this peak recovers in Fig. 3B with the range over which wetting changes are observed in Fig. 2A, it is apparent that wetting changes strongly correlate with the degree of photobleaching. At the onset of partial wetting of water in Fig. 3C (cyan curve, 31.2 J cm^{-2}), the peak at 510 nm (Fig. 3B) has recovered to 98% of its value before p(DR1A-*co*-AA) functionalization. By the time complete wetting of water is observed in Fig. 3C (black curve, 78 J cm^{-2}), this peak has completely recovered.

A similar effect to bulk UV irradiation was also achieved using visible light, however significantly higher illumination doses were required (see ESI†). Although the azobenzene chromophore is generally quite durable with respect to photo-induced damage under normal circumstances,[30] prolonged
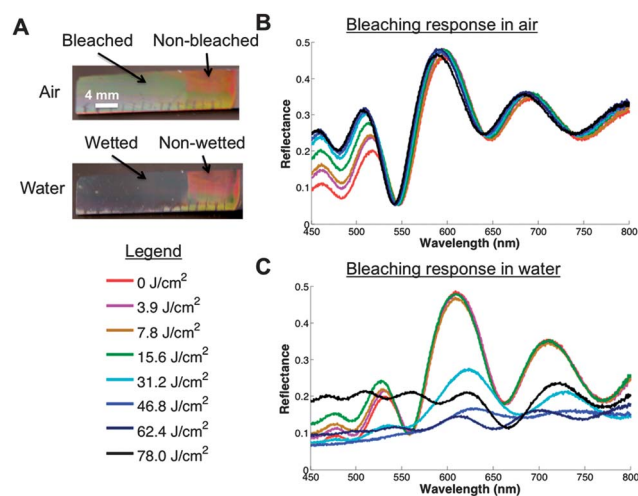

Fig. 3 (A) Images of a p(DR1A-*co*-AA)-functionalized IOF in air (top) and in water (bottom) where photobleaching *via* UV exposure has been applied selectively to the left portion of the film. Comparison of the two images shows that wetting occurs in regions where the chromophore has been photobleached (evidenced by colour contrast in the air image). (B and C) Evolution of the normal incidence reflectance spectra of an IOF region (9 layers thick) in air (B) and submerged in water (C) as a function of UV exposure dose, showing the correlation between photobleaching and the onset of wetting.

exposure to high power densities can have the same photobleaching effect as UV light. Despite higher powers required, using visible light instead of UV light to tune the IOF wetting state may prove useful in applications where UV light would be harmful to other components of a device (*e.g.* dynamically tunable microfluidics). Furthermore, visible-light-induced wettability changes enabled us to induce fluid infiltration *in situ* by irradiating samples while submerged in water (see ESI†).

This technique provides a convenient approach to directly tune the wetting threshold of specific IOF regions to a particular liquid. Thus, a fabrication method using a single functionalization tuned by patterned UV exposure dosages is enabled for colourimetric indicators that mutually distinguish between a large number of liquids.[22,23] Alternatively, as opposed to identifying unknown liquids using wetting patterns in regions with known light exposures, wetting a film with known liquids could be used to colourimetrically identify the amount of prior light exposure in a way that requires no instrumentation. In this mode of operation, such a film could be deposited (*e.g.* on a sticker) onto an outdoor surface or appliance and used as a low-cost monitor of its age (if stored outside). The same principle of operation could be used to design anti-tamper films that indicate if a sealed package has been opened. It is worth noting that the photostability of the azo-chromophore results in a dynamic range of UV-dose sensitivity that is relatively high (corresponding to ∼20 minutes–2 hours of direct sunlight exposure).[31] While this may be ideal for longer term exposure monitoring (*e.g.* age reporting), practical tamper-indicating devices would likely require increased light sensitivity by at least one or two orders of magnitude.

Conclusions

We have shown that the sharply defined wetting threshold in crack-free inverse opal films functionalized with p(DR1A-*co*-AA) can be directly and continuously tuned with light exposure. Exposure of films to UV or visible light increased hydrophilicity, allowing liquids of increasing surface tension to penetrate the pores. These wettability changes, caused by photobleaching of the chromophore, were irreversible, indelibly recording light exposure history in a way that is both highly sensitive and easy to identify. These qualities make this type of material potentially useful as a tamper-indicating seal or a low-cost monitor of material aging.

References

1 I. B. Burgess, M. Lončar and J. Aizenberg, *J. Mater. Chem. C*, 2013, **1**, 6075–6086.

2 Y. Zhao, X. Zhao and Z. Gu, *Adv. Funct. Mater.*, 2010, **20**, 2970–2988.

3 O. C. Farokhzad and R. Langer, *ACS Nano*, 2009, **3**, 16–20.

4 J. Wang and K. M. Manesh, *Small*, 2010, **6**, 338–345.

5 R. P. Wool, *Soft Matter*, 2008, **4**, 400–418.

6 R. J. Mortimer, *Chem. Soc. Rev.*, 1997, **26**, 147–156.

7 M. Kolle, A. Lethbridge, M. Kreysing, J. J. Baumberg, J. Aizenberg and P. Vukusic, *Adv. Mater.*, 2013, **25**, 2239–2245.

8 A. C. Fahrenbach, S. C. Warren, J. T. Incorvati, A.-J. Avestro, J. C. Barnes, J. F. Stoddart and B. A. Grzybowski, *Adv. Mater.*, 2013, **25**, 331–348.

9 A. Coskun, M. Banaszak, R. D. Astumian, J. F. Stoddart and B. Grzybowski, *Chem. Soc. Rev.*, 2011, **41**, 19–30.

10 P.-G. de Gennes, F. Brochard-Wyart and Q. Quere, *Capillarity and wetting phenomena: drops, bubbles, pearls, waves*, Springer, New York, 2004.

11 B. Xin and J. Hao, *Chem. Soc. Rev.*, 2010, **39**, 769–782.

12 X. Yao, Y. Song and L. Jiang, *Adv. Mater.*, 2011, **23**, 719–734.

13 A. Goulet-Hanssens and C. J. Barrett, *J. Polym. Sci., Part A: Polym. Chem.*, 2013, **51**, 3058–3070.

14 M. Yamada, M. Kondo, J. Mamiya, Y. Yu, M. Kinoshita, C. J. Barrett and T. Ikeda, *Angew. Chem., Int. Ed.*, 2008, **47**, 4986–4988.

15 K. Ichimura, S.-K. Oh and M. Nakagawa, *Science*, 2000, **288**, 1624–1626.

16 S.-K. Oh, M. Nakagawa and K. Ichimura, *J. Mater. Chem.*, 2002, **12**, 2262–2269.

17 N. M. Ahmad, M. Saqib and C. J. Barrett, *J. Macromol. Sci., Part A: Pure Appl. Chem.*, 2010, **47**, 534–544.

18 R. Rosario, D. Gust, M. Hayes, F. Jahnke, J. Springer and A. A. Garcia, *Langmuir*, 2002, **18**, 8062–8069.

19 N. M. Ahmad, X. Lu and C. J. Barrett, *J. Mater. Chem.*, 2010, **20**, 244–247.

20 B. Hatton, L. Mishchenko, S. Davis, K. H. Sandhage and J. Aizenberg, *Proc. Natl. Acad. Sci. U. S. A.*, 2010, **107**, 10354–10359.

21 I. B. Burgess, L. Mishchenko, B. D. Hatton, M. Kolle, M. Lončar and J. Aizenberg, *J. Am. Chem. Soc.*, 2011, **133**, 12430–12432.

22 K. P. Raymond, I. B. Burgess, M. H. Kinney, M. Lončar and J. Aizenberg, *Lab Chip*, 2012, **12**, 3666–3669.

23 I. B. Burgess, N. Koay, K. P. Raymond, M. Kolle, M. Lončar and J. Aizenberg, *ACS Nano*, 2012, **6**, 1427–1437.

24 S. J. Yeo, H. Kang, Y. H. Kim, S. Han and P. J. Yoo, *ACS Appl. Mater. Interfaces*, 2012, **4**, 2107–2115.

25 N. M. Ahmad, M. Saqib and C. J. Barrett, *J. Macromol. Sci., Part A: Pure Appl. Chem.*, 2010, **47**, 106–118.

26 G. Vazquez, E. Alvarez and J. M. Navaza, *J. Chem. Eng. Data*, 1995, **40**, 611–614.

27 S. Bian, J. M. Williams, D. Y. Kim, L. Li, S. Balasubramanian, J. Kumar and S. Tripathy, *J. Appl. Phys.*, 1999, **86**, 4498–4508.

28 A. Galvan-Gonzalez, M. Canva, G. I. Stegeman, R. Twieg, T. C. Kowalczyk and H. S. Lackritz, *Opt. Lett.*, 1999, **24**, 1741–1743.

29 A. Galvan-Gonzalez, M. Canva, G. I. Stegeman, L. Sukhomlinova, R. J. Twieg, K. P. Chan, T. C. Kowalczyk and H. S. Lackritz, *J. Opt. Soc. Am. B*, 2000, **17**, 1992–2000.

30 N. C. Holme, P. S. Ramanujam and S. Hvilsted, *Opt. Lett.*, 1996, **21**, 902–904.

31 http://rredc.nrel.gov/solar/spectra/am1.5/, retrieved 30 September, 2013.